Environmental Science & Technology Letters

Letter

pubs.acs.org/journal/estlcu

Sulfate Radical-Induced Disinfection of Pathogenic *Escherichia coli* O157:H7 via Iron-Activated Persulfate

Dawit N. Wordofa,[†] Sharon L. Walker, and Haizhou Liu*

Department of Chemical and Environmental Engineering, University of California, Riverside, California 92521, United States

Supporting Information

ABSTRACT: Sulfate radical ($SO_4^{\bullet-}$) has been increasingly applied as an efficient oxidant for water treatment in recent years. This study investigated the disinfection efficacy of $SO_4^{\bullet-}$ on *Escherichia coli* O157:H7, i.e., a pathogenic strain of *E. coli* on the U.S. Environmental Protection Agency's Contaminant Candidate List. $SO_4^{\bullet-}$ was generated via persulfate ($S_2O_8^{2-}$) activation using ferrous iron (Fe^{2+}). Results showed that $S_2O_8^{2-}$ activation and subsequent $SO_4^{\bullet-}$ exposure induced the loss of pathogenic *E. coli* viability. The disinfection, kinetics exhibited an induction phase followed by a rapid first-order decay phase. Dosages of $S_2O_8^{2-}$ and Fe^{2+} significantly impacted the duration of the induction phase and the rate of disinfection; on the other hand, the solution pH preferentially impacted the induction time, and the dosage of Fe^{3+}-reducing agent hydroxylamine (NH_2OH) impacted the rate of disinfection. The disinfection kinetics depended on the CT equivalence of total $SO_4^{\bullet-}$ exposure. Results showed that $SO_4^{\bullet-}$ exposure initiated the loss of *E. coli* O157:H7 cell viability 5 times faster than $HO^{\bullet}$ exposure did. This unique feature of $SO_4^{\bullet-}$ is possibly associated with its highly selective reactivity with electron-rich moieties on the surface of *E. coli* O157:H7 cell membranes.

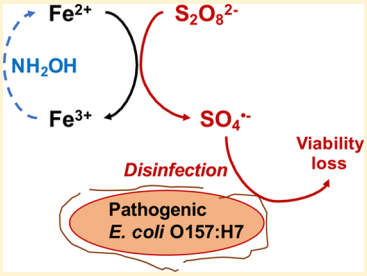

INTRODUCTION

Outbreaks of pathogenic microorganisms in water supplies pose great challenges to public health. Disinfection is a crucial step in water treatment for the destruction of pathogens and protection of public health.[1] Beyond traditional chlorine-based disinfectants, oxidative radicals generated from advanced oxidation processes have been increasingly employed for water treatment. For example, hydroxyl radical ($HO^{\bullet}$), usually generated from hydrogen peroxide (H_2O_2) via Fenton reaction or UV, has been widely applied.[2,3] $HO^{\bullet}$ is effective in bacterial disinfection because its highly oxidative nature allows it to degrade cell lipids, proteins, and nucleic acid, thus creating irreversible oxidative damage to the cell membranes and resulting in a loss of cell viability.[4−6] In recent years, sulfate radical ($SO_4^{\bullet-}$) has also been proposed as an alternative oxidant, because of its strong capacity to degrade recalcitrant organic contaminants.[7−15] $SO_4^{\bullet-}$ is similar to $HO^{\bullet}$ in its oxidative ability but possesses a higher reactivity with electron-rich chemicals.[16] Although the strong oxidative nature of $SO_4^{\bullet-}$ makes it a potentially effective disinfectant, little is known about its disinfection efficacy on pathogenic bacteria.

Prior studies of $SO_4^{\bullet-}$ inactivation mainly focused on marine phytoplankton or nonpathogenic bacteria in drinking water.[17,18] Pathogenic bacteria in a water supply pose a great threat to public health. In particular, *Escherichia coli* O157:H7, a waterborne and highly virulent strain of *E. coli* that produces Shiga-like toxins, is notoriously known worldwide for its outbreaks from drinking water.[19−22] The associated health effects include gastrointestinal illness and hemolytic uremic syndrome.[20,23−25] It was recently placed on the U.S. Environmental Protection Agency's drinking water Contaminant Candidate List (CCL4).[26] Therefore, preventing the occurrence of *E. coli* O157:H7 in water supplies is crucial.[25,27] Furthermore, *E. coli* O157:H7 cells possess a variety of unique external and surface bond macromolecules, including flagella, proteins, and extracellular polymeric substances (EPS).[28−30] These surface characteristics can affect the resistance of *E. coli* O157:H7 to oxidative stress compared to those of other nonpathogenic *E. coli* strains.[30,31]

$SO_4^{\bullet-}$ can be generated via persulfate ($S_2O_8^{2-}$) activation by Fenton reaction, UV irradiation, heat, base, electrodes, and nanoparticles.[32−38] In particular, Fenton reaction is a convenient approach, during which ferrous iron (Fe^{2+}) is added and oxidized by persulfate to ferric iron (Fe^{3+}), while persulfate is activated to $SO_4^{\bullet-}$.[39,40] The solution pH affects the efficiency of iron persulfate activation.[2] To increase the yield of $SO_4^{\bullet-}$, hydroxylamine (NH_2OH) was typically added as a reducing reagent to promote the conversion of ferric iron to its ferrous form.[41−43] However, the nature and potential benefit for the $SO_4^{\bullet-}$-driven disinfection of the pathogenic strain of *E. coli* are still unknown.

The main objective of this study was to investigate the kinetics of $SO_4^{\bullet-}$-induced disinfection of pathogenic *E. coli* O157:H7, using iron persulfate activation to generate $SO_4^{\bullet-}$, and examine its loss of viability with varying solution pH values and concentrations of persulfate, ferrous iron, and hydroxyl-

Received: February 1, 2017
Revised: March 3, 2017
Accepted: March 6, 2017
Published: March 6, 2017

DOI: 10.1021/acs.estlett.7b00035
Environ. Sci. Technol. Lett. 2017, 4, 154−160

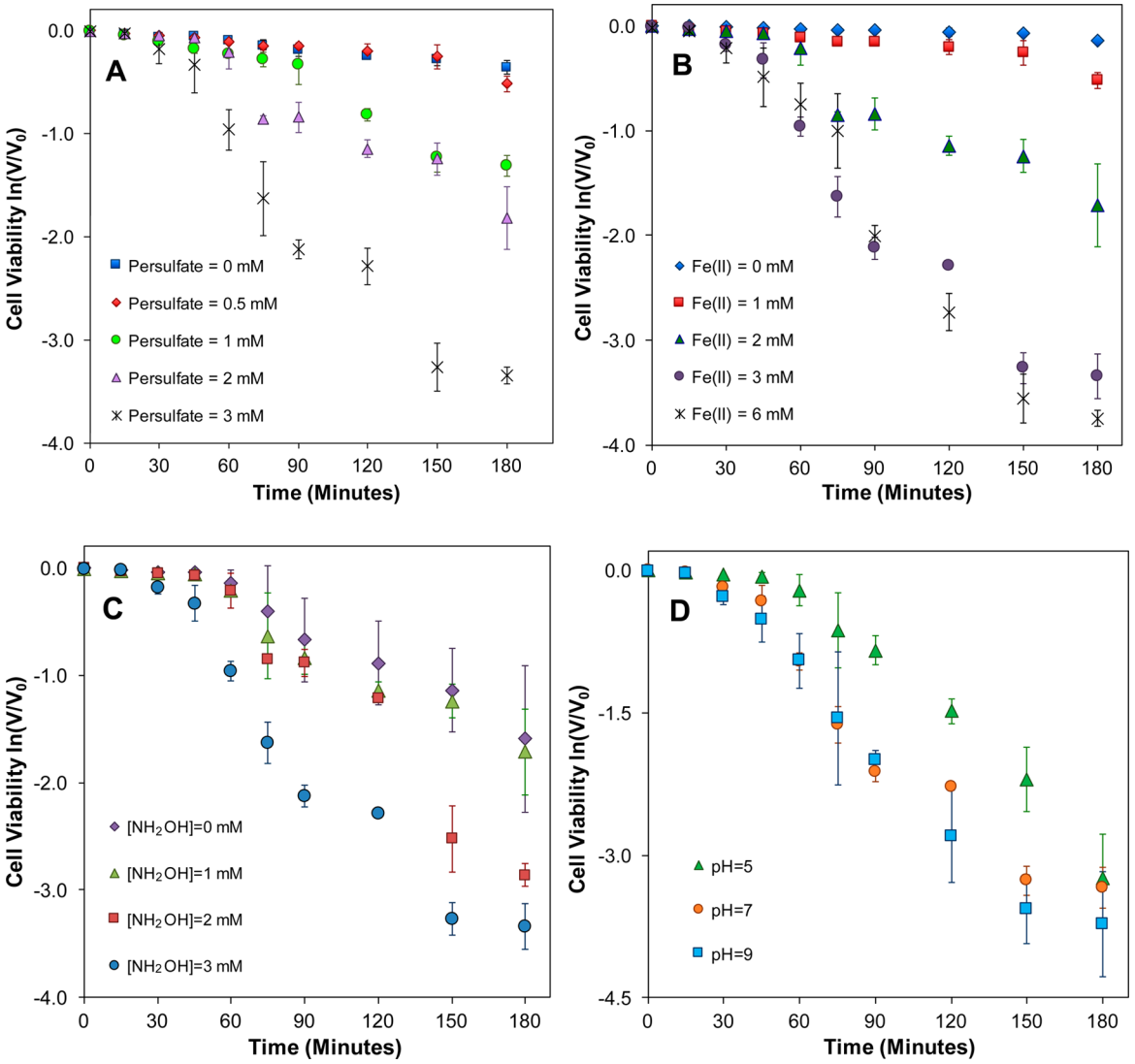

Figure 1. Impact of chemical parameters on the viability of *E. coli* O157:H7 cells during persulfate activation by ferrous iron: (A) persulfate concentration, (B) ferrous iron concentration, (C) hydroxylamine concentration, and (D) solution pH. Unless specified in the figure legend, the experimental condition included 3 mM $S_2O_8^{2-}$, 3 mM Fe(II), 3 mM NH_2OH, and pH 7.

amine. The disinfection kinetics of $SO_4^{\bullet-}$ was also compared to that of $HO^{\bullet}$ based on the total radical exposure.

MATERIALS AND METHODS

All chemicals used in this study were reagent grade. An *E. coli* O157:H7 stock solution was prepared by inoculating the cells from a stock culture overnight at 37 °C. This preculture was then inoculated in a 300 mL LB broth [1:100 (v/v)] for an additional 4 h to reach the exponential growth phase (Figure S1). The concentration of the *E. coli* stock solution was quantified with a cell counting chamber via light microscopy (Micromaster, Fisher Scientific). The final incubated *E. coli* suspension was centrifuged and washed three times with 5 mM KCl to create an *E. coli* stock suspension.

To start a disinfection experiment, a requisite amount of a 100 mM persulfate stock solution prepared from $K_2S_2O_8$ was quickly mixed with a predetermined amount of the *E. coli* stock suspension in a 250 mL sterilized glass batch reactor. The targeted persulfate concentration was varied between 0 and 3 mM. Ferrous iron was added using a freshly prepared 100 mM $FeSO_4$ stock solution to create a Fe^{2+}:$S_2O_8^{2-}$ molar ratio of 0−6. In some experiments, NH_2OH was added to the solution. Phenol at a concentration ranging from 0.3 to 1 mM was added as a probe compound to measure the steady-state $SO_4^{\bullet-}$ concentration in each disinfection experiment.[44] Although a kinetic model is theoretically possible for predicting the radical concentration, the direct probe method can quantify the quasi-steady-state radical concentrations. The solution pH was held constant at the targeted value between 5 and 9 by adding droplets of 50 mM $HClO_4$ or NaOH. The solution ionic strength was held at 25 mM. Similar disinfection experiments were performed with H_2O_2, during which $HO^{\bullet}$ was produced. At each predetermined time interval, 5 μL of a sample was withdrawn from the reactor to measure the viability of *E. coli*, which indicated the loss of cell membrane integrity. An additional 5 mL sample was filtered through a 0.22-μm Millipore filter to measure the concentrations of persulfate and phenol. All experiments were conducted in triplicate at 25 °C.

The viability of *E. coli* was measured using a well-accepted live/dead fluorescent staining assay.[31,45−48] Viable cells exhibited green fluorescence, whereas dead cells showed red fluorescence under a fluorescent microscope (Olympus BX 51).

DOI: 10.1021/acs.estlett.7b00035
Environ. Sci. Technol. Lett. 2017, 4, 154−160

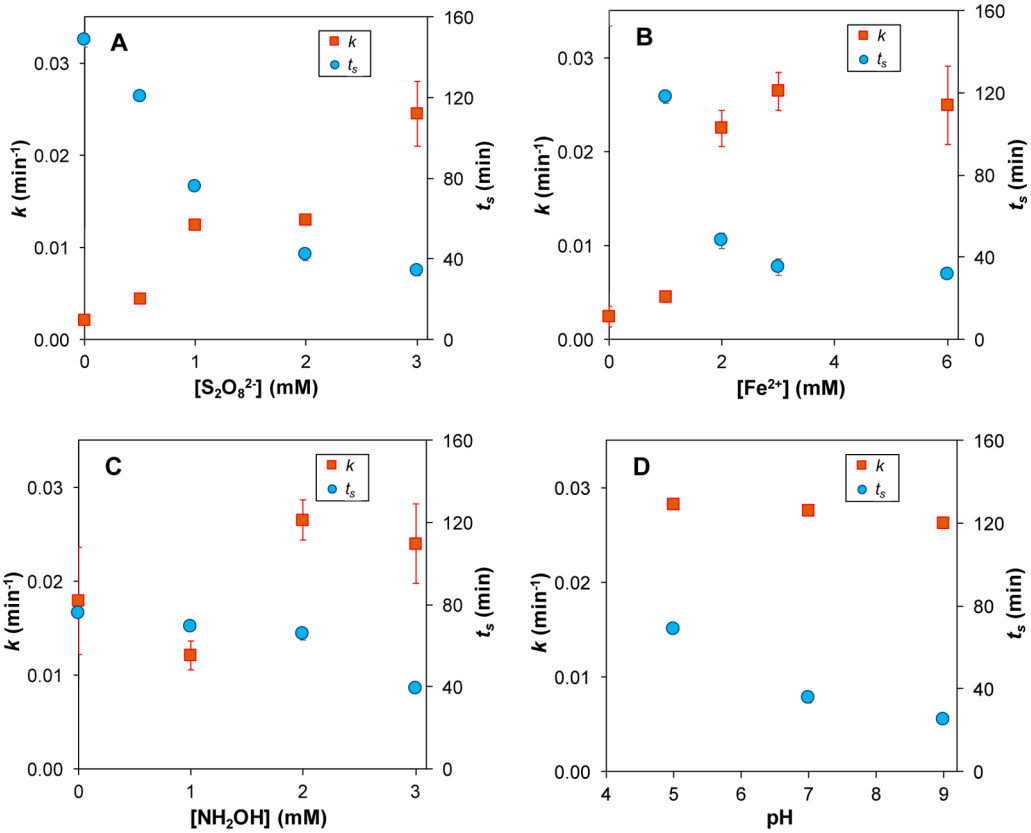

Figure 2. Impact of solution chemical parameters on the induction time (t_s) and viability loss rate constant (k) of *E. coli* O157:H7 disinfection: (A) persulfate concentration, (B) ferrous iron concentration, (C) hydroxylamine concentration, and (D) solution pH. Unless specified in the figure legend, the experimental condition included 3 mM $S_2O_8^{2-}$, 3 mM Fe(II), 3 mM NH_2OH, and pH 7.

Cell viability was calculated as the natural logarithm of the ratio of living cells to total cells. Persulfate was measured using the KI colorimetric method.[49] Phenol was analyzed with an Agilent 1200 high-performance liquid chromatography (HPLC) instrument equipped with a diode array detector at a wavelength of 254 nm.[9]

RESULTS AND DISCUSSION

Loss of *E. coli* Viability during Persulfate Activation. The change in *E. coli* viability exhibited two distinct stages: an initial period of induction time, or a "lag" phase, during which the cell viability exhibited little change; and an ensuing "rapid decay" phase associated with a pronounced loss of viability (Figure 1). The loss of cell viability was also accompanied by the change in the fluorescence of the cells (Figure S2). The persulfate concentration strongly affected the durations of these two phases, while in control experiments without persulfate, *E. coli* cells exhibited a negligible loss of viability throughout the entire duration of exposure (Figure 1A). The concentration of Fe^{2+} impacted both the duration of the lag phase and the rate of the rapid decay phase (Figure 1B). The presence of hydroxylamine also accelerated the loss of cell viability, with a shorter induction time and more rapid decay kinetics at higher hydroxylamine concentrations (Figure 1C). On the other hand, the solution pH did not impact the rate of rapid disinfection kinetics but significantly impacted the induction time, with a higher pH inducing the loss of viability more quickly (Figure 1D).

Kinetics of Disinfection of *E. coli* O157:H7 by $SO_4^{\bullet-}$. To quantitatively describe the loss of *E. coli* cell viability, a multitarget bacterial disinfection model was established to describe the two-phase behavior using eq E1:

$$N = N_0\{1 - [1 - \exp(-kt)]^m\} \quad \text{(E1)}$$

This model has been used to express typical viability loss profiles during disinfection of bacteria and *Crytosporidium parvum* oocysts.[50,51] N is the number of viable bacteria at a particular exposure time. N_0 is the total number of bacteria cells before exposure to the persulfate iron activation system (cells per milliliter). t is the exposure time (minutes). k and m are two intrinsic parameters. k is the inactivation rate constant for the exponential decay phase (inverse minutes). m is an intrinsic model fitting parameter with no physical meaning. The values of k and m were obtained by fitting the model with experimental data using the Matlab software. The induction time (t_s) was defined as the period during which the population of cells exhibited <5% of viability loss; i.e., $N/N_0 < 0.05$. Consequently, t_s was calculated using eq E2:

$$t_s = -\frac{1}{k}\ln\left[1 - \left(\frac{19}{20}\right)^{1/m}\right] \quad \text{(E2)}$$

Values of k and t_s were obtained using the disinfection model (Table S1). Inactivation rate constant k increased almost linearly with the dosage of persulfate, while the induction time and persulfate dosage exhibited an inversely exponential decay relationship (Figure 2A). Rate constant k also increased rapidly with the dosage of Fe^{2+} before plateauing, while the induction time decreased exponentially with Fe^{2+} concentration (Figure 2B). An addition of NH_2OH increased k but only modestly

DOI: 10.1021/acs.estlett.7b00035
Environ. Sci. Technol. Lett. 2017, 4, 154−160

impacted t_s (Figures 2C). In contrast, the solution pH affected k more significantly than the induction time (Figures 2D).

Mechanism of Disinfection by $SO_4^{\bullet-}$. The observed *E. coli* O157:H7 viability loss resulted from the generation of $SO_4^{\bullet-}$ from persulfate activation via a Fenton-like reaction:[52,53]

$$S_2O_8^{2-} + Fe^{2+} \rightarrow SO_4^{\bullet-} + SO_4^{2-} + Fe^{3+} \quad k_1 = 20\ M^{-1}\ s^{-1} \tag{R1}$$

Under typical experimental conditions in this study (i.e., 1−5 mM $S_2O_8^{2-}$, 1−5 mM Fe^{2+}, and pH 7), Fe^{2+} acted as the major sink for $SO_4^{\bullet-}$:[54−56]

$$SO_4^{\bullet-} + Fe^{2+} \rightarrow SO_4^{2-} + Fe^{3+} \quad k_2 = 4.6 \times 10^9\ M^{-1}\ s^{-1} \tag{R2}$$

In addition, $S_2O_8^{2-}$ was a main sink for $HO^{\bullet}$:[32,57−60]

$$HO^{\bullet} + S_2O_8^{2-} \rightarrow S_2O_8^{\bullet-} + HO^- \quad k_3 = 1.4 \times 10^7\ M^{-1}\ s^{-1} \tag{R3}$$

The steady-state concentration of $SO_4^{\bullet-}$ was approximately 2 orders of magnitude higher than that of $HO^{\bullet}$ (details provided in Text S1). Therefore, the generation of $HO^{\bullet}$ from the persulfate system was negligible. Persulfate radical ($S_2O_8^{\bullet-}$) is not an effective oxidant and decayed into inert sulfate and dissolved oxygen.[7,9] Persulfate remained stable without ferrous iron (Fe^{2+}) but quickly decomposed in the presence of Fe^{2+} (Figure S3).

The rapid cell viability losses (i.e., a decrease in t_s) with increasing initial $S_2O_8^{2-}$ and Fe^{2+} concentrations could be attributed to the generation of oxidative $SO_4^{\bullet-}$ (Figure 2A,B). However, because of the scavenging effect of excess Fe^{2+} on $SO_4^{\bullet-}$, the yield of $SO_4^{\bullet-}$ eventually decreased at higher Fe^{2+} concentrations, resulting in a plateau of the values of k and t_s (Figure 2B). The presence of NH_2OH also accelerates the disinfection kinetics. As persulfate was activated, Fe^{3+} was generated (reaction E1). The presence of NH_2OH effectively reduced Fe^{3+} to Fe^{2+}:[41−43]

$$Fe^{3+} + NH_2OH \rightarrow Fe^{2+} + NH_2O^{\bullet} + H^+ \tag{R4}$$

Therefore, the presence of NH_2OH increased the availability of Fe^{2+} and the yield of $SO_4^{\bullet-}$. Consequently, the rate of disinfection increased with NH_2OH dosage (Figure 2C). Intermediate product $NH_2O^{\bullet}$ was further converted to inorganic nitrogen via the reduction of Fe^{3+} to Fe^{2+}.[41−43,61−63]

With regard to solution pH, it impacted the availability of Fe^{2+} for persulfate activation. Fe^{2+} was oxidized by dissolved O_2:[64]

$$Fe^{2+} + \frac{1}{4}O_2 + \frac{5}{2}H_2O \rightarrow Fe(OH)_{3(s)} + 2H^+ \tag{R5}$$

The rate of reaction R3 increased by 8 orders of magnitude when the pH was increased from 5 to 9. Meanwhile, the rate of Fe^{2+} oxidation by $SO_4^{\bullet-}$ (reaction E2) and the rate of Fe^{2+} oxidation by $S_2O_8^{2-}$ (reaction E1) were approximately constant regardless of pH (calculation provided in Text S2). Consequently, as the solution pH increased from 5 to 9, Fe^{2+} was preferentially scavenged by dissolved O_2, and the effect of scavenging of $SO_4^{\bullet-}$ by Fe^{2+} decreased significantly, leading to an increase of the effective yield of $SO_4^{\bullet-}$. Therefore, an increase in solution pH shortened t_s (Figure 2D). However, as Fe^{2+} reacted with dissolved O_2 at higher pH values, the fraction of Fe^{2+} that effectively activated persulfate to $SO_4^{\bullet-}$ decreased. Furthermore, a higher pH likely increased the negative surface charge of *E. coli* bacteria, repulsed $SO_4^{\bullet-}$ from the surface of *E. coli* cells, and consequently reduced the accessibility of $SO_4^{\bullet-}$ to *E. coli* cell membranes. As a result, pH had an insignificant effect on k (Figure 2D).

To compare the $SO_4^{\bullet-}$- and $HO^{\bullet}$-driven disinfection of *E. coli* O157:H7, the cell viability loss was expressed as the total radical exposure based on the classic CT concept of disinfection (i.e., $CT = \int_0^t [radical^{\bullet}]_{ss} t$, Chick−Watson model).[1] Calculation of CT values is provided in Text S3. These two radicals exhibited distinct trends in disinfection kinetics (Figure 3).

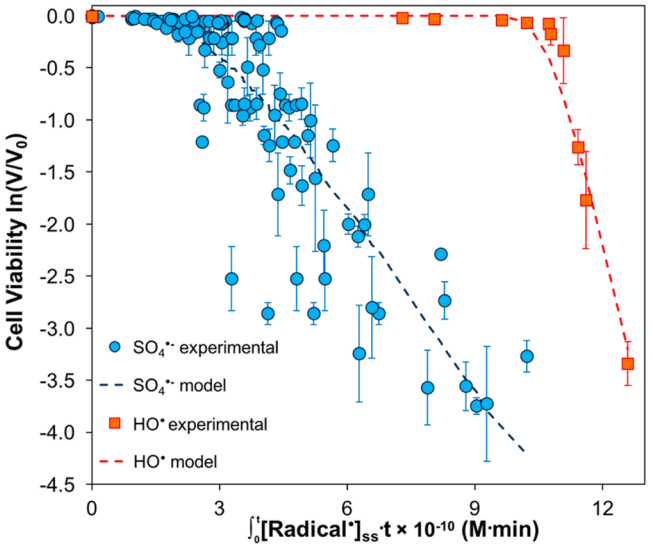

Figure 3. Comparison of $SO_4^{\bullet-}$- and $HO^{\bullet}$-driven disinfection kinetics on *E. coli* O157:H7 on the basis of CT values on radical exposure to iron-activated persulfate. The circles are experimental data. The dashed lines are Chick−Watson model fittings of the experimental data.

$SO_4^{\bullet-}$ induced the loss of *E. coli* O157:H7 cell viability approximately 5 times faster than $HO^{\bullet}$ did, i.e., 2×10^{-10} M min for $SO_4^{\bullet-}$ versus 9.5×10^{-10} M min for $HO^{\bullet}$ based on CT exposure. The data indicate $SO_4^{\bullet-}$ likely had a higher affinity with pathogenic *E. coli* O157:H7 and induced viability loss faster than $HO^{\bullet}$. This unique trend with $SO_4^{\bullet-}$ was not observed with other nonpathogenic *E. coli* strains.[18] It can result from the variation of surface characteristics (e.g., macromolecule level and composition) that have been observed with various *E. coli* isolates.[30] The cell membrane of *E. coli* O157:H7 is surface-bound with macromolecules, including proteins, polysaccharides, and EPS,[28] which could allow the radical oxidation of its cell membrane structure.

$SO_4^{\bullet-}$ selectively reacts with electron-rich organic compounds via a direct electron transfer mechanism, whereas $HO^{\bullet}$ nonselectively reacts with organic compounds via a combination of H abstract and OH addition mechanisms.[16,65] However, once cell viability loss was initiated, $SO_4^{\bullet-}$ exhibited a disinfection rate that was approximately 60% slower than that of $HO^{\bullet}$ (slopes of the two curves in Figure 3). This might be because both *E. coli* bacteria and $SO_4^{\bullet-}$ are negatively charged while $HO^{\bullet}$ is neutral, and $HO^{\bullet}$ was likely more accessible to the surface of bacterial cells once the cell permeability was compromised.[18] The detailed disinfection mechanism will be examined in the future.

Environmental Implications. Results from this study show that iron-activated persulfate can effectively induce the viability loss of pathogenic *E. coli* O157:H7. The disinfection kinetics of $SO_4^{\bullet-}$ exhibits an induction time much shorter than

DOI: 10.1021/acs.estlett.7b00035
Environ. Sci. Technol. Lett. 2017, 4, 154−160

that of $HO^{\bullet}$. Sulfate radical-based disinfection can be implemented in water treatment by adding ferrous iron and persulfate with a desirable contact time, followed by a coagulation/flocculation step to remove the ferric iron hydroxide particles. The disinfection efficiency depends on the control of water chemistry. A desirable dosage of persulfate, ferrous iron can shorten the induction time and enhance the disinfection kinetics. A solution pH in the neutral to basic range and the addition of hydroxylamine can also increase the rate of disinfection. Optimization of these chemical parameters can ensure an efficient yield of sulfate radical and a desirable CT exposure for disinfection. Although this disinfection process generates sulfate as a byproduct, it is a secondary chemical with a U.S. Environmental Protection Agency nonmandatory guideline of 250 mg/L in drinking water. Sulfate formation can be minimized by increasing the stoichiometric yield of sulfate radical from persulfate, e.g., by controlling the optimal dosage of chemicals.

■ ASSOCIATED CONTENT

Supporting Information

The Supporting Information is available free of charge on the ACS Publications website at DOI: 10.1021/acs.estlett.7b00035.

Description of sulfate radical chemistry and figures showing persulfate activation (PDF)

■ AUTHOR INFORMATION

Corresponding Author

*E-mail: haizhou@engr.ucr.edu. Phone: (951) 827-2076. Fax: (951) 827-5696.

ORCID

Haizhou Liu: 0000-0003-4194-2566

Present Address

†D.N.W.: Department of Civil and Environmental Engineering, University of Nevada, Reno, NV 89557.

Notes

The authors declare no competing financial interest.

■ ACKNOWLEDGMENTS

This study was supported by the Faculty Initiation Fund at the University of California (Riverside, CA) and National Science Foundation Grant CHE-1611306. We thank Alicia Taylor, Wei Li, Nicola Kinsinger, and Ian Marcus for assistance on the project.

■ REFERENCES

(1) Crittenden, J. C.; Trussell, R. R.; Hand, D. W.; Howe, K. J.; Tchobanoglous, G. *Water Treatment: Principle and Design*; John Wiley & Sons, Inc.: Hoboken, NJ, 2012.

(2) Pignatello, J. J.; Oliveros, E.; MacKay, A. Advanced oxidation processes for organic contaminant destruction based on the Fenton reaction and related chemistry. *Crit. Rev. Environ. Sci. Technol.* **2006**, *36*, 1−84.

(3) Zhang, R.; Yang, Y.; Huang, C.; Li, N.; Liu, H.; Zhao, L.; Sun, P. UV/H_2O_2 and UV/PDS Treatment of trimethoprim and sulfamethoxazole in synthetic human urine: transformation products and toxicity. *Environ. Sci. Technol.* **2016**, *50* (5), 2573−2583.

(4) Zhang, Y.; Zhou, L.; Zhang, Y.; Tan, C. Inactivation of *Bacillus subtilis* spores using various combination of ultraviolet treatment with addition of hydrogen peroxide. *Photochem. Photobiol.* **2014**, *90*, 609−614.

(5) Cho, M.; Chung, H.; Choi, W.; Yoon, J. Linear correlation between inactivation of *E. coli* and OH radical concentration in TiO_2 photocatalytic disinfection. *Water Res.* **2004**, *38* (4), 1069−1077.

(6) Mamane, H.; Shemer, H.; Linden, K. G. Inactivation of *E. coli*, *B. subtilis* spores, and MS2, T4, and T7 phase using UV/H_2O_2 advanced oxidation. *J. Hazard. Mater.* **2007**, *146* (3), 479−486.

(7) Liu, H.; Bruton, T. A.; Doyle, M. F.; Sedlak, L. D. In situ chemical oxidation of contaminated groundwater by persulfate: decomposition by Fe(III)- and Mn(IV)-containing oxides and aquifer materials. *Environ. Sci. Technol.* **2014**, *48* (17), 10330−10336.

(8) Yang, Q.; Choi, H.; Chen, Y.; Dionysiou, D. D. Heterogeneous activation of peroxymonosulfate by supported cobalt catalysts for the degradation of 2, 4-dichlorophenol in water: the effect of support, cobalt precursor, and UV radiation. *Appl. Catal., B* **2008**, *77* (3), 300−307.

(9) Liu, H.; Bruton, T. A.; Li, W.; Buren, V. J.; Prasse, C.; Doyle, M. F.; Sedlak, L. D. Oxidation of benzene by persulfate in the presence of Fe(III)- and Mn(IV)-containing oxides: stoichiometric efficiency and transformation products. *Environ. Sci. Technol.* **2016**, *50* (2), 890−898.

(10) Fang, G.; Gao, J.; Dionysiou, D. D.; Liu, C.; Zhou, D. Activation of persulfate by quinones: free radical reactions and implication for the degradation of PCBs. *Environ. Sci. Technol.* **2013**, *47* (9), 4605−4611.

(11) Anipsitakis, G. P.; Dionysiou, D. D.; Gonzalez, M. A. Cobalt-mediated activation of peroxymonosulfate and sulfate radical attack on phenolic compounds. Implications of chloride ions. *Environ. Sci. Technol.* **2006**, *40*, 1000−1007.

(12) Yang, Y.; Pignatello, J. J.; Ma, J.; Mitch, W. A. Comparison of halide impacts on the efficiency of contaminant degradation by sulfate and hydroxyl radical-based advanced oxidation processes (AOPs). *Environ. Sci. Technol.* **2014**, *48*, 2344−2351.

(13) Houtz, E. F.; Sedlak, D. L. Oxidative conversion as a means of detecting precursors to perfluoroalkyl acids in urban runoff. *Environ. Sci. Technol.* **2012**, *46*, 9342−9349.

(14) Sra, K. S.; Thomson, N. R.; Barker, J. F. Persistence of persulfate in uncontaminated aquifer materials. *Environ. Sci. Technol.* **2010**, *44*, 3098−3104.

(15) Tsitonaki, A.; Petri, B.; Crimi, M.; Mosbaek, H.; Siegrist, R. L.; Bjerg, P. L. In situ chemical oxidation of contaminated soil and groundwater using persulfate: a review. *Crit. Rev. Environ. Sci. Technol.* **2010**, *40*, 55−91.

(16) Neta, P.; Madhavan, V.; Zemel, H.; Fessenden, R. W. Rate constants and mechanism of reaction of sulfate radical anion with aromatic compounds. *J. Am. Chem. Soc.* **1977**, *99* (1), 163−164.

(17) Ahn, S.; Peterson, T.; Righter, J.; Miles, D.; Tratnyek, P. Disinfection of ballast water with iron activated persulfate. *Environ. Sci. Technol.* **2013**, *47*, 11717−11725.

(18) Sun, P.; Tyree, C.; Huang, C. H. Inactivation of *Escherichia coli*, bacteriophage MS2, and *Bacillus* spores under UV/H_2O_2 and UV/peroxydisulfate advanced disinfection conditions. *Environ. Sci. Technol.* **2016**, *50* (8), 4448−4458.

(19) Swerdlow, D. L.; Woodruff, B. A.; Brady, R. C.; Griffin, P. M.; Tippen, S.; Donnell, H. D., Jr.; Geldreich, E.; Payne, B. J.; Meyer, A., Jr.; Wells, J. G. A Waterborne outbreak in Missouri of *Escherichia coli* O157:H7 associated with bloody diarrhea and death. *Ann. Intern. Med.* **1992**, *117*, 812−819.

(20) Licence, K.; Oates, K. R.; Synge, B. A.; Reid, T. M. An outbreak of *E. coli* O157 infection with evidence of spread from animals to man through contamination of a private water supply. *Epidemiol. Infect.* **2001**, *126*, 135−138.

(21) Olsen, S. J.; Miller, G.; Breuer, T.; Kennedy, M.; Higgins, C.; Walford, J.; McKee, G.; Fox, K.; Bibb, W.; Mead, P. A Waterborne outbreak of *Escherichia coli* O157:H7 infections and hemolytic uremic syndrome: implications for rural water systems. *Emerging Infect. Dis.* **2002**, *8*, 370−375.

(22) Kim, H. N.; Hong, Y.; Lee, I.; Bradford, S. A.; Walker, S. L. Surface characteristics and adhesion behavior of *Escherichia coli* O157:H7: role of extracellular macromolecules. *Biomacromolecules* **2009**, *10*, 2556−2564.

DOI: 10.1021/acs.estlett.7b00035
Environ. Sci. Technol. Lett. 2017, 4, 154−160

(23) O'Brien, A. D.; Newland, J. W.; Miller, S. F.; Holmes, R. K.; Smith, H. W.; Formal, S. B. Shiga-like toxin-converting phages from *Escherichia coli* strains that cause hemorrhagic colitis or infantile diarrhea. *Science* **1984**, *226* (4675), 694−696.
(24) Kaper, J. B.; Karmali, M. A. The continuing evolution of a bacterial pathogen. *Proc. Natl. Acad. Sci. U. S. A.* **2008**, *105*, 4535−4536.
(25) Nwachuku, N.; Gerba, C. P. Occurrence and persistence of *Escherichia coli* O157:H7 in water. *Rev. Environ. Sci. Bio/Technol.* **2008**, *7*, 267−273.
(26) U.S. Environmental Protection Agency. Contaminant Candidate List (CCL) and Regulation Determination. Final CCL4Microbial Contaminants. 2016. https://www.epa.gov/ccl/microbial-contaminants-ccl-4 (accessed February 22, 2017).
(27) Rangel, J. M.; Sparling, P. H.; Crowe, C.; Griffin, P. M.; Swerdlow, D. L. Epidemiology of *Escherichia coli* O157:H7 outbreaks, United States, 1982−2002. *Emerging Infect. Dis.* **2005**, *11*, 603−609.
(28) Law, D. Virulence factors of *Escherichia coli* O157 and other Shiga toxin-producing E. coli. *J. Appl. Microbiol.* **2000**, *88*, 729−745.
(29) Ryu, J. H.; Beuchat, L. R. Biofilm formation by *Escherichia coli* O157:H7 on stainless steel: effect of exopolysaccharide and curli production on its resistance to chlorine. *Appl. Environ. Microbiol.* **2005**, *71* (1), 247−254.
(30) Bolster, C. H.; Cook, K. L.; Marcus, I. M.; Haznedaroglu, B. Z.; Walker, S. L. Correlating transport behavior with cell properties for eight porcine *Escherichia coli.* isolates. *Environ. Sci. Technol.* **2010**, *44*, 5008−5014.
(31) Gong, A. S.; Lanzl, C. A.; Cwiertny, D. M.; Walker, S. L. Lack of influence of extracellular polymeric substances (EPS) level on hydroxyl radical mediated disinfection of *Escherichia coli*. *Environ. Sci. Technol.* **2012**, *46*, 241−249.
(32) Yuan, S.; Liao, P.; Alshawabkeh, A. N. Electrolytic manipulation of persulfate reactivity by iron electrodes for trichloroethylene degradation in groundwater. *Environ. Sci. Technol.* **2014**, *48* (1), 656−663.
(33) Hori, H.; Yamamoto, A.; Hayakawa, E.; Taniyasu, S.; Yamashita, N.; Kutsuna, S.; Kiatagawa, H.; Arakawa, R. Efficient decomposition of environmentally persistent perfluorocarboxylic acids by use of persulfate as a photochemical oxidant. *Environ. Sci. Technol.* **2005**, *39* (7), 2383−2388.
(34) Lau, T. K.; Chu, W.; Graham, N. J. D. The aqueous degradation of butylated hydroxyanisole by UV/$S_2O_8^{2-}$: study of reaction mechanisms via dimerization and mineralization. *Environ. Sci. Technol.* **2007**, *41* (2), 613−619.
(35) Antoniou, M. G.; De La Cruz, A. A.; Dionysiou, D. D. Intermediates and reaction pathways from the degradation of microcystin-LR with sulfate radicals. *Environ. Sci. Technol.* **2010**, *44* (19), 7238−7244.
(36) Liang, C.; Guo, Y. Mass transfer and chemical oxidation of naphthalene particles with zerovalent iron activated persulfate. *Environ. Sci. Technol.* **2010**, *44* (21), 8203−8208.
(37) Liang, C.; Bruell, C. J.; Marley, M. C.; Sperry, K. L. Persulfate oxidation for in situ remediation of TCE. II. Activated by chelated ferrous ion. *Chemosphere* **2004**, *55* (9), 1225−1233.
(38) Johnson, R. L.; Tratnyek, P. G.; Johnson, R. O. Persulfate persistence under thermal activation conditions. *Environ. Sci. Technol.* **2008**, *42*, 9350−9356.
(39) Anipsitakis, G. P.; Dionysiou, D. D. Dionysiou. Degradation of organic contaminants in water with sulfate radicals generated by the conjunction of peroxymonosulfate with cobalt. *Environ. Sci. Technol.* **2003**, *37*, 4790−4797.
(40) Arnold, S. M.; Hickey, W. J.; Harris, R. F. Degradation of atrazine by Fenton's reagent: condition optimization and product quantification. *Environ. Sci. Technol.* **1995**, *29* (8), 2083−2089.
(41) Zou, J.; Ma, J.; Chen, L.; Li, X.; Guan, Y.; Xie, P.; Pan, C. Rapid acceleration of ferrous iron/peroxymonosulfate oxidation of organic pollutants by promoting Fe(III)/Fe(II) cycle with hydroxylamine. *Environ. Sci. Technol.* **2013**, *47*, 11685−11691.
(42) Chen, L.; Li, X.; Zhang, J.; Fang, J.; Huang, Y.; Wang, P.; Ma, J. Production of hydroxyl radical via the activation of hydrogen peroxide by hydroxylamine. *Environ. Sci. Technol.* **2015**, *49*, 10373−10379.
(43) Bengtsson, G.; Fronaeus, S.; Bengtsson-Kloo, L. The kinetics and mechanism of oxidation of hydroxylamine by iron(III). *J. Chem. Soc.-Dalton Trans.* **2002**, *12*, 2548−2552.
(44) Ahmad, M.; Teel, A.; Watts, R. Mechanism of persulfate activation by phenols. *Environ. Sci. Technol.* **2013**, *47*, 5864−5871.
(45) Taylor, A.; Chowdhury, I.; Gong, A. S.; Cwiertny, D. M.; Walker, S. L. Deposition and disinfection of *Escherichia coli* O157:H7 on naturally occurring photoactive materials in a parallel plate chamber. *Environ. Sci. Process. Impact.* **2014**, *16* (2), 194−202.
(46) Ouyang, K.; Dai, K.; Walker, S. L.; Huang, Q.; Yin, X.; Cai, P. Efficient photocatalytic disinfection of *Escherichia coli* O157:H7 using C_{70}-TiO_2 hybrid under visible Light Irradiation. *Sci. Rep.* **2016**, *6*, 25702.
(47) Fauss, E. F.; MacCuspie, R. I.; Oyanedel-Craver, V.; Smith, J. A.; Swami, N. S. Disinfection action of electrostatic versus steric-stabilized silver nanoparticles on *E. coli* under different water chemistries. *Colloids Surf., B* **2014**, *113* (1), 77−84.
(48) Huang, G.; Xia, D.; An, T.; Ng, T. W.; Yip, H. Y.; Li, G.; Zhao, H.; Wong, P. K. Dual roles of capsular extracellular polymeric substances in photocatalytic inactivation of *Escherichia coli*: comparison of *E. coli* BW25113 and isogenic mutants. *Appl. Environ. Microbiol.* **2015**, *81* (15), 5174−5183.
(49) Liang, C.; Huang, C. F.; Mohanty, N.; Kurakalva, R. M. A rapid spectrophotometric determination of persulfate anion in ISCO. *Chemosphere* **2008**, *73*, 1540−1543.
(50) Wegelin, M.; Canonica, S.; Mechsner, K.; Fleischmann, T.; Pesaro, F.; Metzler, A. Solar water disinfection: Scope of the process and analysis of radiation experiments. *J. Water Supply: Res. Technol.—AQUA* **1994**, *43* (4), 154−169.
(51) Rennecker, J. L.; Kim, J. H.; Corona-Vasquez, B.; Mariñas, B. J. Role of disinfectant concentration and pH in the inactivation kinetics of *Crytosporidium parvum* oocysts with ozone and monochloramine. *Environ. Sci. Technol.* **2001**, *35*, 2752−2757.
(52) Sra, K.; Thomson, N.; Barker, J. Persistence of Persulfate in Uncontaminated Aquifer Materials. *Environ. Sci. Technol.* **2010**, *44*, 3098−3104.
(53) Waldemer, R.; Tratnyek, P.; Johnson, R.; Nurmi, J. Oxidation of chlorinated ethenes by heat-activated persulfate: kinetics and products. *Environ. Sci. Technol.* **2007**, *41*, 1010−1015.
(54) Kolthoff, I. M.; Miller, I. K. The chemistry of persulfate. I. The kinetics and mechanism of the decomposition of the persulfate ion in aqueous medium. *J. Am. Chem. Soc.* **1951**, *73* (7), 3055−3059.
(55) Herrmann, H.; Reese, A.; Zellner, R. Time-resolved UV/VIS diode-array absorption spectroscopy of SO_x^- (x = 3, 4, 5) radical anions in aqueous solution. *J. Mol. Struct.* **1995**, *348*, 183−186.
(56) Peyton, G. R. The free-radical chemistry of persulfate-based total organic carbon analyzer. *Mar. Chem.* **1993**, *41*, 91−103.
(57) Zhang, T.; Zhu, H.; Croué, J. P. Production of sulfate radical from peroxymonosulfate induced by a magnetically separable $CuFe_2O_4$ spinel in water: efficiency, stability and mechanism. *Environ. Sci. Technol.* **2013**, *47*, 2784−2791.
(58) Buxton, G. V.; Greenstock, C. L.; Helman, W. P.; Ross, A. B. Critical review of rate constants for reactions of hydrated electrons, hydrogen atoms and hydroxyl radicals ($^{\bullet}OH/^{\bullet}O^-$) in aqueous solution. *J. Phys. Chem. Ref. Data* **1988**, *17*, 513−886.
(59) Das, T. N. Reactivity and role of $SO_5^{\bullet-}$ radical in aqueous medium chain oxidation of sulfite to sulfate and atmospheric sulfuric acid generation. *J. Phys. Chem. A* **2001**, *105*, 9142−9155.
(60) Travina, O. A.; Kozlov, V. N.; Purmal, A. P.; Rod'ko, I. Y. Synergism of the action of the sulfate oxidation initiators, iron and peroxydisulfate ions. *Russ. J. Phys. Chem.* **1999**, *73*, 1215−1219.
(61) Lind, J.; Merenyi, G. Kinetic and thermodynamic properties of the aminoxyl ($NH_2O^{\bullet}$) radical. *J. Phys. Chem. A* **2006**, *110* (1), 192−197.

DOI: 10.1021/acs.estlett.7b00035
Environ. Sci. Technol. Lett. 2017, 4, 154−160

(62) Gowland, R. J.; Stedman, G. Kinetic and product studies on the decomposition of hydroxylamine in nitric acid. *J. Inorg. Nucl. Chem.* **1981**, *43* (11), 2859−2862.
(63) Johnson, M. D.; Hornstein, B. J. The kinetics and mechanism of the ferrate (VI) oxidation of hydroxylamines. *Inorg. Chem.* **2003**, *42* (21), 6923−6928.
(64) Stumm, W.; Morgan, J. J. Kinetics of redox process. *Aquatic Chemistry: Chemical Equilibria and Rates in Natural Waters*; John Wiley & Sons, Inc.: New York, 1996; Chapter 11.
(65) Grebel, J. E.; Pignatello, J. J.; Mitch, W. A. Effect of halide ions and carbonates on organic contaminant degradation by hydroxyl radical-based advanced oxidation processes in saline waters. *Environ. Sci. Technol.* **2010**, *44* (17), 6822−6828.

DOI: 10.1021/acs.estlett.7b00035
Environ. Sci. Technol. Lett. 2017, 4, 154−160